

PARTIALLY SINTERED LEAD-FREE CERAMICS FROM PIEZOELECTRIC POWDERS PREPARED VIA CONVENTIONAL FIRING AND SPARK PLASMA SINTERING (SPS) – – CHARACTERIZATION OF MICROSTRUCTURE AND DIELECTRIC PROPERTIES

[#]KATEŘINA ZLOUŽEOVÁ*, SOŇA HŘÍBALOVÁ*, VOJTĚCH NEČINA*, WILLI PABST*,
MARTIN MÍKA*, JAN PETRÁŠEK**

^{*}Department of Glass and Ceramics, University of Chemistry and Technology, Prague (UCT Prague),
Technická 5, 166 28 Prague, Czech Republic

^{**}Faculty of Electrical Engineering, Czech Technical University (CTU),
Technická 2, 166 27 Prague, Czech Republic

[#]E-mail: katerina.zlouzeova@vscht.cz

Submitted August 8, 2020; accepted October 7, 2020

Keywords: Lead-free piezoelectrics, Potassium sodium niobate (KNN), Barium titanate (BT), Dielectric constant (relative permittivity), Dielectric function, Electrical properties, Partial sintering, Porosity, Spark plasma sintering (SPS)

This work deals with dielectric properties of lead-free ceramics from piezoelectric powders and focuses on the preparation and characterization of potassium-sodium niobate ($K_{0.5}Na_{0.5}NbO_3$, KNN) and barium titanate ($BaTiO_3$, BT) ceramics. Ceramic samples with different porosity were prepared from commercial KNN and BT powders by conventional firing in air or spark plasma sintering (SPS) at temperatures 600 - 1000 °C for KNN and 900 - 1300 °C for BT, resulting in partially or fully sintered microstructures. Bulk density, apparent density and open porosity were determined using the Archimedes method and closed and total porosities were calculated on the basis of theoretical densities. For both types of ceramics, the porosity decreases with increasing sintering temperature, and for identical temperatures the porosity of SPS samples is lower than for conventional firing, because the pressure applied during SPS promotes densification. For KNN the influence of SPS on the porosity is much larger than for BT. With increasing SPS temperature KNN exhibits a moderate decrease of the alkali content. The results of dielectric property measurements and their frequency dependence via impedance spectroscopy in the range from 10 or 100 Hz to 1 MHz show that the relative permittivity decreases in all cases with frequency and is usually higher for ceramics prepared via SPS than for conventional firing. This can be explained by the lower porosity and smaller grain size. The absolute values of the relative permittivity at 1 kHz are 134 - 532 (conventional firing) and 148 - 3780 (SPS) for KNN, and 753 - 1801 (conventional firing) and 923 - 10 380 (SPS) for BT ceramics.

INTRODUCTION

The piezoelectric effect was first discovered by brothers Pierre and Jacques Curie in 1880 in a quartz single crystal [1-4]. The Curie brothers noticed that when stress was applied to quartz crystals, an electric charge was generated on their surface, an effect that was later called the direct piezoelectric effect [2, 3]. The opposite effect, in which the crystal creates a stress proportional to the applied electric field is called the converse piezoelectric effect and was predicted by Gabriel Lippmann in 1881 [1, 2]. The development of piezoelectric materials continued at the beginning of the First World War. At that time, the only available materials, for which the piezoelectric effect was discovered, were the single crystals of quartz and Rochelle salt (sodium potassium tartrate tetrahydrate $KNaC_4H_4O_6 \cdot 4H_2O$). However, their properties were not completely satisfying. Therefore, after World War I, further efforts were made in order to

discover alternative piezoelectric materials with better properties. For example, in 1935 Busch and Scherrer discovered the piezoelectric properties of potassium dihydrogen phosphate KH_2PO_4 [2, 3]. During World War II several research groups independently discovered the ferroelectric properties of barium titanate [2, 3, 5]. Subsequently, the piezoelectric effect for barium titanate was verified by Gray in 1946 [2], and thus – due to its ferroelectric properties – barium titanate became the first piezoelectric material that could be produced in polycrystalline (ceramic) form. However, in 1954, Jaffe and his coworkers discovered a ceramic material with much better piezoelectric properties than barium titanate: ceramics based on lead zirconate titanate $Pb(Zr,Ti)O_3$ [6], so-called PZT ceramics. Thanks to its excellent piezoelectric properties, PZT ceramics are still the most widely used piezoelectric material today [1]. It is clear, however, that the toxicity of lead contained in this ceramic is gradually preventing its further use [4, 7, 8].

Thus, there is an increasing interest in finding alternative lead-free materials with comparably good piezoelectric properties. Current research interests are mainly focused on lead-free materials based on crystallites with perovskite structure, such as potassium sodium niobate $K_xNa_{1-x}NbO_3$ (KNN), barium titanate $BaTiO_3$ (BT) and other BT-based ceramics, sodium bismuth titanate $Bi_{0.5}Na_{0.5}TiO_3$ (BNT) and bismuth ferrite $BiFeO_3$ (BFO). The recently revived research interest in BT ceramics is quite remarkable in this context.

Piezoelectric materials are widely used in electro-technical devices as sensors [9], energy harvesters [10, 11], actuators [4, 12], transducers (e.g. electroacoustic transducers in smartphones, laptops, as speakers and buzzers [4] or as hydrophones – underwater sonars [5, 9, 13-16,]), in high energy applications (e.g. ultrasonic cleaning [4]), medical imaging devices (diagnostic equipment) [17] and in devices for the non-destructive testing of materials [14, 15].

Usually, in the preparation of these materials, an effort is made to achieve the highest possible density [18-21], since, for example, the elastic, dielectric and piezoelectric properties decrease with increasing porosity (pore volume fraction) [18-22]. However, in some cases porosity can be an advantage. In particular, the decrease in relative permittivity with increasing porosity increases the values of some figures of merit, which describe the response rate of a piezoelectric transducer [14, 23]. Porous ceramics can thus show a significant improvement in properties, for example for the application of hydrophones [22, 24], even if, for example, the piezoelectric properties are worse than for their dense counterparts.

This work deals with the preparation of lead-free ceramics from commercially available piezoelectric powders – potassium sodium niobate (KNN) and barium titanate (BT) – by conventional firing and spark plasma sintering (SPS), with the specific intention to prepare these ceramics in partially sintered (i.e. porous) form. The relative permittivity is then measured by impedance spectroscopy in the range from 10 Hz to 1 MHz. The aim of this work is to compare the properties of ceramics samples prepared by conventional firing and SPS.

EXPERIMENTAL

Raw materials

The raw materials used for sample preparation were commercially available powders of potassium sodium niobate (CerPoTech, Norway, with particle size $< 1 \mu m$), and barium titanate (US Research Nanomaterials, USA, with 99.9 % purity and particle size 200 nm). Beside these powders, only polyethylene glycol (PEG 8000, ALDRICH Chemistry) was used as a binder for the preparation of granulates which were subsequently used for uniaxial pressing.

Sample preparation

Based on typical firing temperatures for both KNN and BT ceramics, a wider range of temperatures was selected with a purpose to prepare partially sintered, i.e. porous, ceramics. The samples were prepared by conventional firing (KV) and by spark plasma sintering (SPS).

Uniaxial pressing and conventional firing

Both powders of KNN and BT ceramics were mixed with 5 wt. % PEG and with deionized water, stirred on a laboratory shaker for 24 hours and then dried (in a laboratory oven) at 100 °C for 24 hours. The granulate was then compressed with a manual hydraulic press into cylindrical tablets with diameter 12.7 mm using pressures of 94 MPa for KNN and 110 MPa for BT ceramics.

For samples of KNN ceramics a temperature range of 600 - 1000 °C with steps of 50 °C was chosen, and for samples of BT ceramics a temperature range of 900 - 1300 °C with steps of 100 °C was chosen. The samples were fired for 2 hours in an electrically heated furnace (Nabertherm, Germany) in air with a heating rate of 2 °C·min⁻¹ and with an uncontrolled cooling rate.

SPS method

In spark plasma sintering (SPS), a temperature range of 600 - 1000 °C with steps of 100 °C was chosen for KNN ceramics and a temperature range of 900 - 1300 °C with steps of 100 °C for BT ceramics. The samples were sintered under vacuum in a graphite mold with an internal diameter of 20 mm in a SPS furnace (HP D 10-SD, FCT Systeme, Germany) with a heating rate of 100 °C·min⁻¹, using an initial pressure of 10 MPa, which was raised to 80 MPa after reaching the maximum temperature. The dwell time at maximum temperature was 5 min. The cooling rate was 50 °C·min⁻¹ to the temperature of 600 °C, then 30 °C·min⁻¹ to 300 °C and then uncontrolled.

Characterization

The bulk density, apparent density and open porosity were determined by the Archimedes method. The relative density ρ_r , which was subsequently used for calculating the total porosity ϕ , was directly obtained from knowledge of the theoretical densities ρ_0 4.64 g·cm⁻³ for KNN [25] and 6.01 g·cm⁻³ for BT [26]. The chemical composition was determined by X-ray fluorescence analysis (XRF) on the XRF spectrometer ARL 9400 XP (Thermo ARL, Switzerland) to determine whether KNN was depleted of alkaline elements K and Na during sintering. The analysis was performed for KNN ceramics samples prepared by the SPS method. The dielectric properties of the samples thus prepared and characterized were subsequently measured via impedance spectroscopy. The measurement was performed at various

Table 1. List of workplaces, instruments and parameters for dielectric measurements of samples; (1) – UCT Prague, Department of Inorganic Technology, (2) – CTU, Faculty of Electrical Engineering, (3) – UCT Prague, Department of Glass and Ceramics.

| | (1) | (2) | (3) | (3) |
|-----------------------|---|----------------|-------------------|--------------------------|
| Instrument | Solartron Frequency Response Analyser SI 1250 | FLUKE PM6306 | Autolab PGSTAT 30 | MOTECH MT 4090 LCR Meter |
| Arrangement | Three-point | Two-point | Two-point | Two-point |
| Frequency range (Hz) | 65 000 – 0.01 | 1 000 000 – 50 | 1 000 000 – 1 | 200 000 – 100 |
| Voltage amplitude (V) | 0.02 | 1 | 0.5 | 0.25 / 1 |

workplaces and on various instruments, the list of which, together with the measurement parameters, is summarized in Table 1. All dielectric measurements were performed at room temperature.

The following relations (from [27]) were used to calculate the real and imaginary part of the relative permittivity from the primary data (real and imaginary part of the impedance) measured by impedance spectroscopy:

$$\varepsilon' = \frac{t}{\omega A \varepsilon_0} \frac{Z}{Z'^2 + Z''^2} \quad (1)$$

$$\varepsilon'' = \frac{t}{\omega A \varepsilon_0} \frac{Z'}{Z'^2 + Z''^2} \quad (2)$$

where A is the cross-sectional area of the sample, t the thickness of the sample, ε_0 the vacuum permittivity, Z' the real part of the impedance, Z'' the imaginary part of the impedance, ε'_r the real part of the relative permittivity and ε''_r the imaginary part of the relative permittivity.

The following relationship [27] was then used to calculate the loss tangent $\tan \delta$:

$$\tan \delta = \frac{\varepsilon''_r}{\varepsilon'_r} \quad (3)$$

RESULTS

Bulk density, apparent density and porosity

KNN ceramics

Basic microstructural parameters (bulk density ρ , apparent density ρ_A , open porosity ϕ_{open} , closed porosity ϕ_{closed} and total porosity ϕ) are given in Tables 2 and 3 for the samples of KNN ceramics prepared by SPS and KV, respectively.

For KNN ceramics prepared by SPS, there is evidently an increase in the bulk density ρ and a decrease in the open porosity ϕ_{open} and the total porosity ϕ with increasing sintering temperature. On the other hand, the apparent density, being in the range of 4.37 - 4.46 g·cm⁻³, does not differ very much for the different sintering temperatures, which indicates that the proportion of closed porosity remains approximately constant as soon as a certain minimum sintering temperature is exceeded.

For KNN ceramics prepared by conventional firing (KV) an increase in bulk density and a decrease in apparent and total porosity can also be observed with increasing firing temperature, but the trend is less pronounced, and the absolute values are at a lower level. The apparent density is in the range of 4.31 - 4.43 g·cm⁻³, so its value increases slightly with the firing temperature, but also in this case the proportion of closed porosity remains approximately constant.

Table 2. Basic microstructural parameters for samples of KNN ceramics prepared by SPS.

| T (°C) | ρ (g·cm ⁻³) | ρ_A (g·cm ⁻³) | ϕ_{open} (%) | ϕ_{closed} (%) | ϕ (%) |
|-------------|---------------------------------|-----------------------------------|-----------------------------|-------------------------------|---------------|
| 600 | 2.57 | 4.37 | 0.412 | 0.034 | 0.446 |
| 700 | 3.15 | 4.40 | 0.285 | 0.037 | 0.322 |
| 800 | 4.01 | 4.46 | 0.099 | 0.036 | 0.135 |
| 900 | 4.41 | 4.43 | 0.005 | 0.045 | 0.050 |
| 1000 | 4.44 | 4.46 | 0.006 | 0.038 | 0.044 |

Table 3. Basic microstructural parameters for samples of KNN ceramics prepared by KV.

| T (°C) | ρ (g·cm ⁻³) | ρ_A (g·cm ⁻³) | ϕ_{open} (%) | ϕ_{closed} (%) | ϕ (%) |
|-------------|---------------------------------|-----------------------------------|-----------------------------|-------------------------------|---------------|
| 650 | 2.42 | 4.31 | 0.438 | 0.040 | 0.478 |
| 700 | 2.43 | 4.32 | 0.438 | 0.039 | 0.477 |
| 750 | 2.46 | 4.35 | 0.434 | 0.035 | 0.469 |
| 800 | 2.28 | 4.38 | 0.479 | 0.029 | 0.508 |
| 850 | 2.55 | 4.39 | 0.420 | 0.031 | 0.451 |
| 900 | 2.45 | 4.39 | 0.443 | 0.030 | 0.473 |
| 950 | 2.69 | 4.42 | 0.390 | 0.029 | 0.419 |
| 1000 | 2.98 | 4.43 | 0.327 | 0.030 | 0.358 |

It is evident that for comparable firing or sintering temperatures the total porosities of samples prepared by SPS are much lower than for samples prepared by KV (e.g. samples fired at temperatures of 700, 800, 900 and 1000 °C have porosities 32, 14, 5 and 4 % for SPS and 48, 51, 47 and 36 % for KV). This is of course due to the pressure applied in SPS. The applied pressure is responsible for the much greater (and faster) densification at a given temperature.

BT ceramics

Basic microstructural parameters (bulk density ρ , apparent density ρ_A , open porosity ϕ_{open} , closed porosity ϕ_{closed} and total porosity ϕ) are given in Tables 4 and 5 for the samples of BT ceramics prepared by SPS and by KV, respectively.

As with KNN ceramics, for BT ceramics prepared by either SPS or KV an increase in bulk density ρ can be observed with increasing sintering temperature, indicating higher densification and decreasing total porosity ϕ and open porosity ϕ_{open} with increasing sintering temperature. Again, the apparent density ρ_A and thus also the proportion of closed porosity is approximately constant for all samples, irrespective of the sintering temperature.

Table 4. Basic microstructural parameters for samples of BT ceramics prepared by SPS.

| T (°C) | ρ (g·cm ⁻³) | ρ_A (g·cm ⁻³) | ϕ_{open} (1) | ϕ_{closed} (1) | ϕ (1) |
|-------------|---------------------------------|-----------------------------------|-----------------------------|-------------------------------|---------------|
| 900 | 3.61 | 5.92 | 0.390 | 0.009 | 0.399 |
| 1000 | 4.58 | 5.95 | 0.230 | 0.008 | 0.238 |
| 1100 | 5.47 | 5.77 | 0.051 | 0.039 | 0.090 |
| 1200 | 5.93 | 5.98 | 0.009 | 0.005 | 0.014 |
| 1300 | 5.97 | 5.99 | 0.003 | 0.004 | 0.007 |

Table 5. Basic microstructural parameters for samples of BT ceramics prepared by KV.

| T (°C) | ρ (g·cm ⁻³) | ρ_A (g·cm ⁻³) | ϕ_{open} (1) | ϕ_{closed} (1) | ϕ (1) |
|-------------|---------------------------------|-----------------------------------|-----------------------------|-------------------------------|---------------|
| 900 | 3.51 | 5.92 | 0.406 | 0.009 | 0.415 |
| 1000 | 3.76 | 5.95 | 0.369 | 0.006 | 0.375 |
| 1100 | 4.38 | 5.97 | 0.266 | 0.005 | 0.271 |
| 1200 | 5.42 | 5.65 | 0.041 | 0.058 | 0.099 |
| 1300 | 5.90 | 5.94 | 0.007 | 0.011 | 0.019 |

X-ray fluorescence analysis

X-ray fluorescence (XRF) analysis was performed for the KNN ceramic samples prepared by SPS, in order to determine the elemental composition after sintering to different temperatures. For the purpose of comparison XRF analysis was also performed for the original

Table 6. Composition of oxides in the original KNN powder ("Raw") and in samples of KNN ceramics prepared by SPS at different temperatures.

| T (°C) | Na ₂ O (wt. %) | K ₂ O (wt. %) | Nb ₂ O ₅ (wt. %) |
|-------------|------------------------------|-----------------------------|---|
| Raw | 10.68 | 13.33 | 75.99 |
| 600 | 9.62 | 13.13 | 77.25 |
| 700 | 9.34 | 12.74 | 77.92 |
| 800 | 9.01 | 12.84 | 78.15 |
| 900 | 9.47 | 13.06 | 77.48 |
| 1000 | 9.58 | 12.81 | 77.61 |

as-supplied KNN powder (designated as "Raw"). Table 6 lists the mass contents of sodium, potassium and niobium oxides for the different sintering temperatures and for the original KNN powder.

The detected mass fractions of alkali metal oxides in the KNN ceramics and their comparison with the original KNN powder indicate that during the SPS process there is a slight decrease in Na₂O content (from the original 10.7 wt. % to values in the range of 9.0 - 9.6 wt. %), but the difference between the individual sintering temperatures seems to be negligible (e.g. the value of 9.6 wt. % correspond to both the lowest firing temperature of 600 °C and the highest 1000 °C).

Also in the case of K₂O, a slight decrease can be observed (from the original 13.3 wt. % to values in the range of 12.7 - 13.1 wt. %), but compared to Na₂O this decrease seems to be almost negligible, probably because the potassium is considerably larger and thus less mobile than the sodium ion. Although information about the volatility of Na₂O and K₂O often appears in the literature and is mentioned as a problem in the preparation of KNN ceramics [28], in our case the XRF analysis revealed that alkalis volatilize only in very small amounts during the SPS process. With respect to the fact that SPS works in vacuum, this might seem surprising, but on the other hand one has to take into account the fact that also the processing times are relatively short in SPS, which might be a major factor preventing volatilization (which is of course kinetically governed by the diffusion rates).

Impedance spectroscopy

For selected samples impedance spectroscopy measurements have been performed on four different instruments. However, systematic characterization of all samples has been performed only on two instruments, MOTECH and Autolab. While the first of these provides data only for a few selected frequencies, the latter yields the complete frequency dependence of the complex dielectric function. Therefore, all graphs shown in this section are based on data from the Autolab instrument. Results of all other measurements are summarized in Tables 7-10.

From the measured data, the values for the real parts of the relative permittivity ϵ'_r , the imaginary parts of the relative permittivity ϵ''_r and the tangent loss $\tan \delta$ (all depending on the frequency) were calculated using Equations 1-3.

KNN ceramics

The dependence of the real part of the relative permittivity ϵ'_r on the frequency for the Autolab instrument is shown in Figure 1. It can be seen that samples of KNN ceramics prepared by SPS usually have higher values compared to samples prepared by conventional firing, which is in line with the literature: due to faster heating rate and shorter dwell time of the samples at maximum

temperature during the SPS process, excessive grain growth is suppressed. It is known that the dielectric properties are dependent on the grain size (the smaller the grains, the higher the relative permittivity due to the high resistivity of the grain boundary [19-22]). This was confirmed for most samples, with the exception of the SPS 1000 sample, where it shows very low ϵ_r' values, but this was probably an artefact caused by degradation of the silver electrode during the measurements.

Overall, it can be stated that in the samples of KNN ceramics the real parts of the relative permittivity ϵ_r' show clearly decreasing trends with increasing frequency. Absolute values (only for Solartron, FLUKE and Autolab, as the MOTECH results deviated from trends) range between 6580 - 32 900 for SPS and 411 - 2144 for KV at a frequency of 10 Hz and between 60 - 132 for SPS and 53 - 104 for KV at a frequency of 1 MHz.

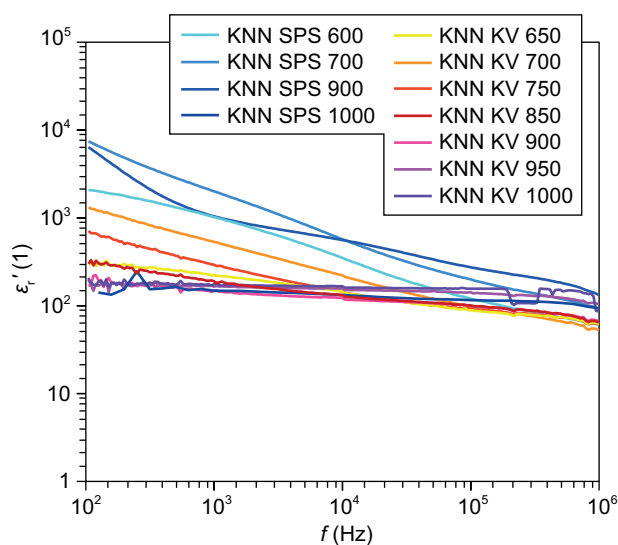


Figure 1. Dependence of ϵ_r' on frequency for samples of KNN ceramics (Autolab).

The dependence of the imaginary part of the relative permittivity ϵ_r'' on the frequency for the Autolab instrument is shown in Figure 2. The values of ϵ_r'' are usually higher for the samples prepared by SPS (except for the sample SPS 1000, probably for the reason mentioned above in the context of ϵ_r').

The frequency dependence of the loss tangent $\tan \delta$ is shown in Figure 3. Actually, for this quantity the measurements provide results without any significant frequency dependence. The values of loss tangent are in the range of 0.03 - 0.96 for samples prepared by KV and slightly larger (0.09 - 1.56) for samples prepared by SPS.

The values ϵ_r' , ϵ_r'' and $\tan \delta$ for frequencies 1, 10, 100 kHz are summarized in the tables, for samples of KNN ceramics prepared by SPS in Table 7 and for samples of KNN ceramics prepared by KV in Table 8. It can be seen that the values of ϵ_r' , ϵ_r'' and $\tan \delta$ are higher for samples prepared by SPS.

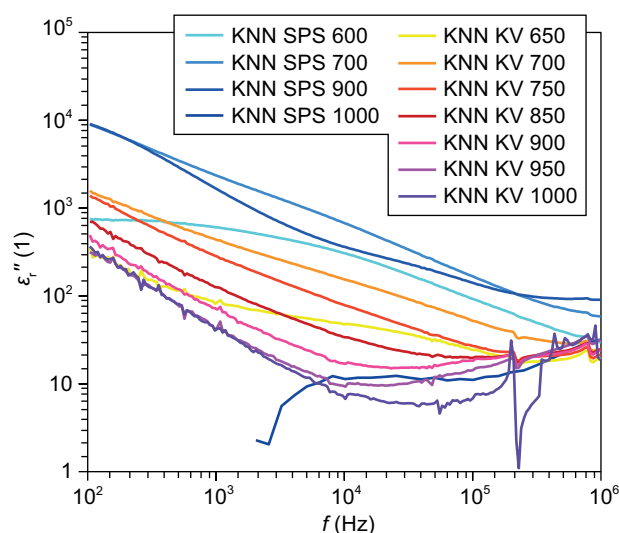


Figure 2. Dependence of ϵ_r'' on frequency for samples of KNN ceramics (Autolab).

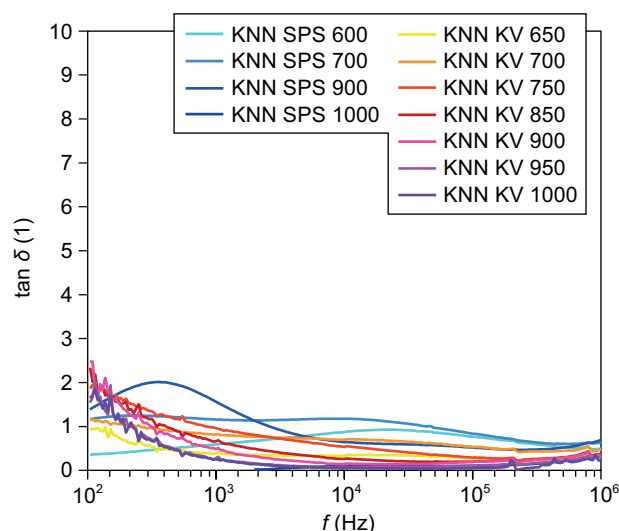


Figure 3. Dependence of $\tan \delta$ on frequency for samples of KNN ceramics (Autolab).

Table 7. Range of values of ϵ_r' , ϵ_r'' and $\tan \delta$ for different frequencies measured on different instruments for samples of KNN ceramics prepared by SPS.

| Apparatus | f (kHz) | ϵ_r' (1) | ϵ_r'' (1) | $\tan \delta$ (1) |
|-----------|--------------|----------------------|-----------------------|----------------------|
| Solartron | 1 | 1090-3780 | 767-4110 | 0.70-2.98 |
| FLUKE | | 832-2263 | 355-2716 | 0.32-1.20 |
| Autolab | | 148-2004 | 603-2320 | 0.59-1.56 |
| MOTECH | | 3-1178 | 15-2827 | 0.07-23.24 |
| Solartron | 10 | 521-1210 | 221-1060 | 0.31-1.20 |
| FLUKE | | 126-795 | 153-552 | 0.74-1.31 |
| Autolab | | 132-571 | 11-669 | 0.09-1.17 |
| MOTECH | | 30-678 | 2-856 | 0.08-5.22 |
| Solartron | 100 | — | — | — |
| FLUKE | | 61-691 | 37-142 | 0.11-0.61 |
| Autolab | | 115-273 | 11-141 | 0.10-0.84 |
| MOTECH | | 5-293 | 11-244 | 0.12-5.33 |

Table 8. Range of values of ε_r' , ε_r'' and $\tan \delta$ for different frequencies measured on different instruments for samples of KNN ceramics prepared by KV.

| Apparatus | f (kHz) | ε_r' (1) | ε_r'' (1) | $\tan \delta$ (1) |
|-----------|--------------|-------------------------|--------------------------|----------------------|
| Solartron | 1 | 233-507 | 38-797 | 0.16-1.57 |
| FLUKE | | 134-219 | 17-111 | 0.13-0.60 |
| Autolab | | 146-532 | 42-432 | 0.24-0.96 |
| MOTECH | | 14-624 | 9-503 | 0.24-3.79 |
| Solartron | 10 | 152-256 | 21-182 | 0.40-0.71 |
| FLUKE | | 104-123 | 4-64 | 0.03-0.60 |
| Autolab | | 122-221 | 7-154 | 0.04-0.69 |
| MOTECH | | 14-159 | 12-278 | 0.08-9.83 |
| Solartron | 100 | – | – | – |
| FLUKE | | 69-119 | 3-33 | 0.2-0.48 |
| Autolab | | 89-156 | 7-52 | 0.04-0.53 |
| MOTECH | | 20-123 | 70-117 | 0.74-5.76 |

BT ceramics

The dependence of the real part of the relative permittivity ε_r' on the frequency for the Autolab instrument is shown in Figure 4. It can be seen that all KV samples, and in addition the SPS 900 and 1000 samples, show a similar course of frequency dependence with a slightly decreasing trend (and with an indication of increasing permittivity values with increasing sintering temperature, i.e. with decreasing porosity), while the SPS 1100, 1200 and 1300 show a qualitatively significantly different course (with a strong frequency dependence), which must be related to a relatively low porosity (0.7 - 9.0 %) in combination with a relatively small grain size. Absolute values obtained with the Autolab instrument decrease from 1104 - 27277 for SPS and 766 - 1541 for KV at a frequency of 100 Hz to 57 - 229 for SPS and 392 - 848 for KV at a frequency of 1 MHz, see Tables 9-10.

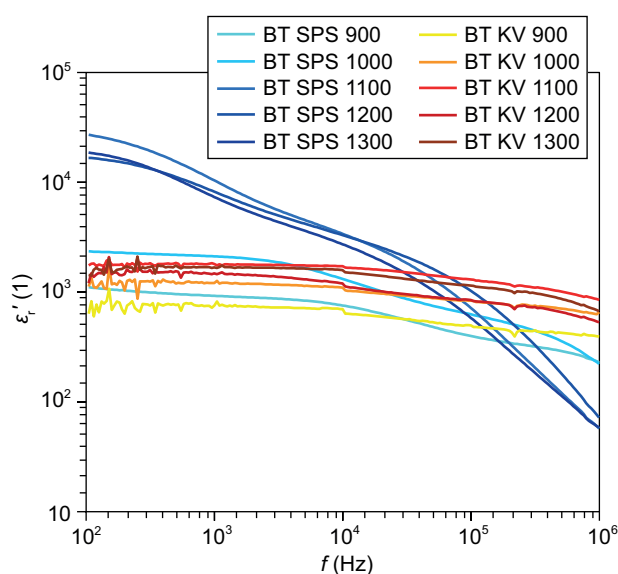


Figure 4. Dependence of ε_r' on frequency for samples of BT ceramics (Autolab).

The dependence of the imaginary part of the relative permittivity ε_r'' on the frequency for the Autolab instrument is shown in Figure 5. From the frequency dependences of the imaginary part of the relative permittivity it can be concluded that the values corresponding to the samples obtained by SPS at a sufficiently high temperature (1100 - 1300 °C) are orders of magnitude higher than those of the samples prepared by KV.

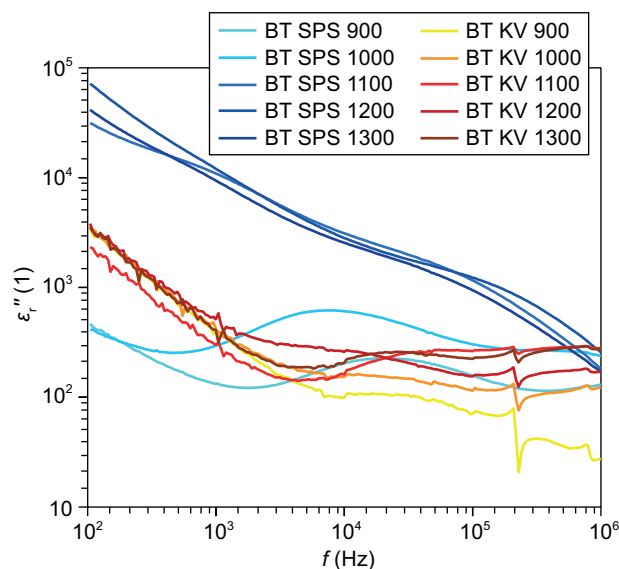


Figure 5. Dependence of ε_r'' on frequency for samples of BT ceramics (Autolab).

The dependence of the loss tangent $\tan \delta$ on the frequency for the Autolab instrument is shown in Figure 6. The values of loss tangent for samples of BT ceramics (measured with the Autolab instrument) range approximately between 0.0 - 5.0 (i.e. significantly larger than for KNN ceramics) and it seems that the course of the curve is similar for all samples.

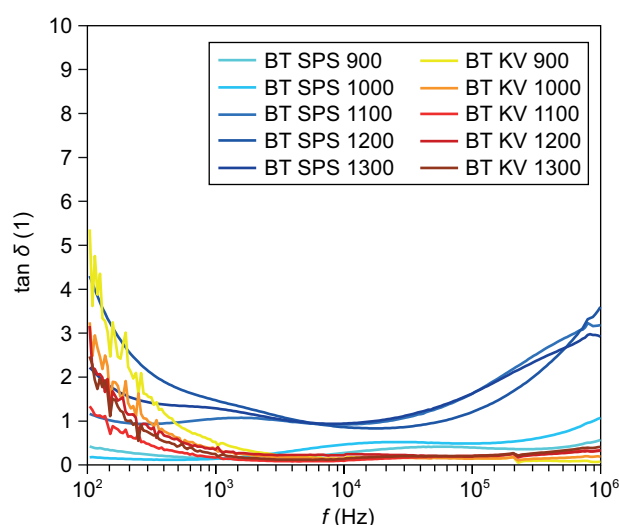


Figure 6. Dependence of $\tan \delta$ on frequency for samples of BT ceramics (Autolab).

The values ε'_r , ε''_r and $\tan \delta$ for frequencies 1, 10, 100 kHz are summarized in the tables, for samples of BT ceramics prepared by SPS in Table 9 and for samples of BT ceramics prepared by KV in Table 10. In comparison with the KNN ceramics prepared in this work, these values are significantly higher for the BT ceramics. For the sample prepared by SPS at a temperature of 1300 °C, a surprisingly high value of ε'_r was achieved at a frequency of 1000 Hz – 10380.

Table 9. Range of values of ε'_r , ε''_r and $\tan \delta$ for different frequencies measured on different instruments for samples of BT ceramics prepared by SPS.

| Apparatus | f (kHz) | ε'_r (1) | ε''_r (1) | $\tan \delta$ (1) |
|-----------|--------------|-------------------------|--------------------------|----------------------|
| Autolab | 1 | 923-10380 | 132-12005 | 0.14-1.47 |
| MOTECH | | 127-23285 | 694-21619 | 0.39-129.82 |
| Autolab | 10 | 755-3385 | 203-3107 | 0.27-0.94 |
| MOTECH | | 22-6718 | 764-5875 | 0.87-35.42 |
| Autolab | 100 | 398-1024 | 157-1225 | 0.39-1.62 |
| MOTECH | | 41-1441 | 385-1916 | 1.02-17.66 |

Table 10. Range of values of ε'_r , ε''_r and $\tan \delta$ for different frequencies measured on different instruments for samples of BT ceramics prepared by KV.

| Apparatus | f (kHz) | ε'_r (1) | ε''_r (1) | $\tan \delta$ (1) |
|-----------|--------------|-------------------------|--------------------------|----------------------|
| Autolab | 1 | 753-1801 | 300-511 | 0.17-0.52 |
| MOTECH | | 466-4918 | 66-14110 | 0.1-3.29 |
| Autolab | 10 | 700-1716 | 98-258 | 0.09-0.22 |
| MOTECH | | 159-9135 | 584-6691 | 0.56-3.81 |
| Autolab | 100 | 498-1298 | 70-263 | 0.14-0.20 |
| MOTECH | | 227-1259 | 151-791 | 0.12-3.48 |

CONCLUSION

This work dealt with the dielectric properties of lead-free ceramics from piezoelectric powders, namely the preparation and characterization of potassium sodium niobate ($\text{K}_{0.5}\text{Na}_{0.5}\text{NbO}_3$, KNN) and barium titanate (BaTiO_3 , BT) ceramics. In the experimental part of this work, ceramics samples were prepared from commercial KNN and BT powders by conventional firing and spark plasma sintering (SPS) with a wide range of temperatures in order to prepare partially sintered (porous) ceramics. It should be emphasized that the ceramic samples prepared and characterized in this work are not piezoelectric, because the process of “poling” was not applied.

Bulk density, apparent density, open porosity, closed porosity and total porosity of the prepared samples were determined by the Archimedes method. It is clear that for both KNN and BT the bulk density increases

(and the open and total porosity decreases) with increasing sintering temperature (while the apparent density remains approximately constant, indicating a relatively constant volume fraction of closed porosity). For the samples of KNN ceramics it was observed that for the same sintering temperatures, the total porosity of the samples prepared by SPS is always significantly lower than for samples prepared by conventional firing, because the pressure applied during the SPS process promotes densification. Compared to BT, the effect of the use of SPS on the porosity of the prepared samples is significantly greater for KNN. This is probably related to the fact that in the case of KNN the application of pressure has a significantly greater effect on compaction than in the case of BT, which may be due to a different sintering mechanism.

The chemical composition of KNN samples prepared by SPS and the original KNN powder was determined by X-ray fluorescence analysis. This analysis was performed only for KNN, because in literature there is often a reference to the volatility of alkali oxides during firing. But as the SPS temperature increases, only a very slight decrease in the alkali content could be observed, so that alkali volatilization does not appear to be a significant complication in the preparation of KNN ceramics by SPS.

Measurements of dielectric properties and their frequency dependence by impedance spectroscopy were performed on four different instruments (at three different workplaces). For the samples of KNN ceramics it was found that the real and imaginary parts of relative permittivity show a decreasing trend and the results show that the absolute values of relative permittivity are higher for samples prepared by SPS (compared to samples prepared by conventional firing), which is caused by the higher densification in the SPS process and thus the lower porosity of the samples. The loss tangent for the samples of KNN ceramics do not have a clear trend with frequency for all samples, but the values are generally higher for the samples prepared by SPS. The frequency dependence of the real part of the relative permittivity for the samples of BT ceramics is also decreasing. The real part of the relative permittivity for samples SPS 1100, 1200 and 1300 shows (in contrast to samples prepared by conventional firing and samples SPS 900 and 1000) a strong frequency dependence, which may be due to relatively low porosity and small grain size. The frequency dependence of the imaginary part of the relative permittivity of BT prepared by SPS at a sufficiently high temperature (1100 - 1300 °C) attains values that are higher by orders of magnitude compared to samples by SPS at a lower temperature and compared to samples prepared by conventional firing. The frequency dependence of the loss tangent shows a very similar course for all BT samples. Similar to KNN, also for BT ceramics the loss tangent values are higher for samples prepared by SPS.

Acknowledgement

This work is part of the project “Partially and fully sintered ceramics – preparation, microstructure, properties, modelling and theory of sintering” (GA18-17899S) supported by Czech Science Foundation (Grantová agentura České republiky/GAČR). The authors would like to thank Ing. Simona Randáková (Central Laboratories, UCT Prague) for the X-ray fluorescence analyses and especially Ing. Michaela Plevová, Ing. Jaromír Hnát, Ph.D., doc. Ing. Martin Paidar, Ph.D. (Department of Inorganic Technology, UCT Prague) for making the first test measurements for this work on the Solartron instrument.

REFERENCES

- Jaffe B., Cook W.R., Jaffe H. (1971). *Piezoelectric Ceramics*. Academic Press Inc.
- Uchino K. (2010). *Advanced Piezoelectric Materials: Science and Technology*. 1st ed. Woodhead.
- von Hippel A. (1994). *Dielectrics and Waves*. 2nd ed. Artech House.
- Zheng T., Wu, J., Xiao D., Zhu J. (2018): Recent development in lead-free perovskite piezoelectric bulk materials. *Progress in Materials Science*, 98, 552-624. doi: 10.1016/j.pmatsci.2018.06.002
- Tichý J., Erhart J., Kittinger E., Přívratská J. (2010). *Fundamentals of Piezoelectric Sensorics: Mechanical, Dielectric, and Thermodynamical Properties of Piezoelectric Materials*. Springer.
- Jaffe B., Roth, R.S., Marzullo S. (1954): Piezoelectric properties of lead zirconate-lead titanate solid-solution ceramics. *Journal of Applied Physics*, 25, 809-810. doi: 10.1063/1.1721741
- Ibn-Mohammed T., Koh S.C.L., Reaney I.M., Acquaye A., Wang D., Taylor S., Genovese A. (2016): Integrated hybrid life cycle assessment and supply chain environmental profile evaluations of lead-based (lead zirconate titanate) versus lead-free (potassium sodium niobate) piezoelectric ceramics. *Energy & Environmental Science*, 9, 3495-3520. doi: 10.1039/c6ee02429g
- Song H.C., Cho K.H., Park H.Y., Ahn C.W., Nahm S., Uchino K., Park S.H., Lee H.G. (2007): Microstructure and piezoelectric properties of $(1-x)(\text{Na}_{0.5}\text{K}_{0.5})\text{NbO}_{3-x}\text{LiNbO}_3$ ceramics. *Journal of the American Ceramic Society*, 90, 1812-1816. doi: 10.1111/j.1551-2916.2007.01698.x
- Nesterov A.A., Topolov V.Y., Tolstunov M.I., Isaeva A.N. (2019): Improved piezoelectric performance and hydrostatic parameters of a novel 2-0-2-0 composite. *Materials Letters*, 252, 158-160. doi: 10.1016/j.matlet.2019.05.104
- Coondoo I., Panwar N., Kholkin A. (2013): Lead-free piezoelectrics: Current status and perspectives. *Journal of Advanced Dielectrics*, 03, 1330002-1-1330002-22. doi: 10.1142/s2010135x13300028
- Roscow J.I., Pearce H., Khanbareh H., Kar-Narayan S., Bowen C.R. (2019): Modified energy harvesting figures of merit for stress- and strain-driven piezoelectric systems. *The European Physical Journal Special Topics*, 228, 1537-1554. doi: 10.1140/epjst/e2019-800143-7
- Hofmann D.P. (2015). *Solid State Physics: An Introduction*. 2nd ed. Wiley-VCH
- Gibiansky L.V., Torquato S. (1997): On the use of homogenization theory to design optimal piezocomposites for hydrophone applications. *Journal of the Mechanics and Physics of Solids*, 45, 689-708. doi: 10.1016/S0022-5096(96)00106-8
- Nelli Silva E.C., Ono Fonseca J. S., Kikuchi N. (1997): Optimal design of piezoelectric microstructures. *Computational Mechanics*, 19, 397-410. doi: 10.1007/s004660050188
- Pabst W. (2020): Effective properties of porous piezoelectric ceramics (in preparation).
- Piazza D., Galassi C., Barzegar A., Damjanovic D. (2008): Dielectric and piezoelectric properties of PZT ceramics with anisotropic porosity. *Journal of Electroceramics*, 24, 170-176. doi: 10.1007/s10832-008-9553-8
- Lee J.-K. (2005): An analytical study on prediction of effective properties in porous and non-porous piezoelectric composites. *Journal of Mechanical Science and Technology*, 19, 2025-2031. doi: 10.1007/BF02916495
- Hoshina T., Takizawa K., Li J., Kasama T., Kakemoto H., Tsurumi T. (2008): Domain size effect on dielectric properties of barium titanate ceramics. *Japanese Journal of Applied Physics*, 47, 7607-7611. doi: 10.1143/jjap.47.7607
- Maiwa H. (2008): Preparation and properties of BaTiO₃ ceramics by spark plasma sintering. *Japanese Journal of Applied Physics*, 47, 7646-7649. doi: 10.1143/jjap.47.7646
- Takeuchi T., Tabuchi M., Kageyama H. (1999): Preparation of dense BaTiO₃ ceramics with submicrometer grains by spark plasma sintering. *Journal of American Ceramic Society*, 82, 939-943. doi: 10.1111/j.1151-2916.1999.tb01857.x
- Yang W.G., Zhang B.P., Ma N., Zhao L. (2012): High piezoelectric properties of BaTiO₃-xLiF ceramics sintered at low temperatures. *Journal of the European Ceramic Society*, 32, 899-904. doi: 10.1016/j.jeurceramsoc.2011.10.054
- Kar-Gupta R., Venkatesh T. (2006): Electromechanical response of porous piezoelectric materials. *Acta Materialia*, 54, 4063-4078. doi: 10.1016/j.actamat.2006.04.037
- Iyer S., Venkatesh T.A. (2011): Electromechanical response of (3-0) porous piezoelectric materials: effects of porosity shape. *Journal of Applied Physics*, 110, 034109-1-034109-8. doi: 10.1063/1.3622509
- Dunn M.L., Taya M. (1993): Electromechanical properties of porous piezoelectric ceramics. *Journal of American Ceramic Society*, 76, 697-706. doi: 10.1111/j.1151-2916.1993.tb06637.x
- Kuscer D., Kocjan A., Majcen M., Meden A., Radan K., Kovač J., Malič B. (2019): Evolution of phase composition and microstructure of sodium potassium niobate – based ceramic during pressure-less spark plasma sintering and post-annealing. *Ceramics International*, 45, 10429-10437. doi: 10.1016/j.ceramint.2019.02.102
- Shen Z.Y., Li, J.F. (2010): Enhancement of piezoelectric constant d_{33} in BaTiO₃ ceramics due to nano-domain structure. *Journal of the Ceramic Society of Japan*, 118, 940-943. doi: 10.2109/jcersj2.118.940
- Joshi J. H., Kanchan D. K., Joshi M. J., Jethva H. O., Parikh K. D. (2017): Dielectric relaxation, complex impedance and modulus spectroscopic studies of mix phase rod like cobalt sulfide nanoparticles. *Materials Research Bulletin*, 93, 63-73. doi: 10.1016/j.materresbull.2017.04.013
- Priya S., Nahm S. (2012). *Lead-Free Piezoelectrics*. Springer.